

1 **Psychophysiological interaction and beta series correlation for task modulated connectivity:**  
2 **modeling considerations and their relationships**

3

4 Xin Di <sup>1,2</sup>, Zhiguo Zhang <sup>3,4</sup>, Bharat B Biswal <sup>1,2\*</sup>

5 1, School of Life Sciences and Technology, University of Electronic Science and Technology of China,  
6 Chengdu, China

7 2, Department of Biomedical Engineering, New Jersey Institute of Technology, Newark, NJ, 07029, USA

8 3, School of Biomedical Engineering, Health Science Center, Shenzhen University, Shenzhen, China

9 4, Guangdong Provincial Key Laboratory of Biomedical Measurements and Ultrasound Imaging,  
10 Shenzhen, China

11

1    **Abstract**

2    Psychophysiological interaction (PPI) and beta series correlations (BSC) are two commonly used  
3    methods for studying task modulated connectivity using functional MRI (fMRI) data. So far there are no  
4    comprehensive tutorials to explain these two methods, and the relationships between these two have not  
5    been established. In the current paper, we explain in detail what the two methods measure, and how these  
6    two methods are related. We demonstrate that the PPI approach always measures connectivity  
7    differences as coded in the psychological variable. We further establish that putting some conditions of  
8    no-interest as 0 does not mean to “zero out” those conditions, but introduces arbitrary effects regarding to  
9    these conditions. However, if modeled correctly, direct contrast PPI with conditions of no-interest  
10   modeled as 0 can generate the same results as the “generalized PPI” approach. In contrast to PPI, the  
11   BSC approach can measure absolute connectivity in a specific condition. When comparing different  
12   conditions, PPI and BSC methods could in principle generate similar results. We also report PPI and  
13   BSC analyses on empirical fMRI data of a stop signal task to illustrate our points.

14

15   **Keywords:** Beta series, Deconvolution, Event-related design, Functional connectivity,  
16   Psychophysiological interaction.

17

18

## 1 **1. Introduction**

2 Although the majority of fMRI studies are task-based, because of its simplicity, resting-state fMRI has  
3 emerged as an alternative method to measure functional connectivity (Biswal et al., 1995, 2010). The  
4 entire scan period of resting-state can be treated as a single state. Therefore, correlation coefficients of  
5 time series between different brain regions could be used to study functional connectivity (Biswal et al.,  
6 1995). For task based fMRI, there are typically multiple task conditions within a scan. The challenge is  
7 to estimate functional connectivity differences between different conditions. There are primarily two  
8 methods that have been developed to study functional connectivity differences for task fMRI data, namely  
9 psychophysiological interaction (PPI) (Friston et al., 1997) and beta series correlation (BSC) (Rissman et  
10 al., 2004). There is also dynamic causal modeling (DCM) that can be used for this purpose (Friston et al.,  
11 2003). However, this method is restricted to a small number of regions of interest, and is largely  
12 hypothesis-driven. Therefore, we did not cover DCM in the current paper.

13 PPI was first proposed by Friston and colleagues based on interaction terms in a regression model  
14 (Friston et al., 1997). After it was initially proposed, a major update was made to perform deconvolution  
15 on the time series from the seed region, so that the interaction term could be calculated at the “neuronal  
16 level” rather than at the hemodynamic response level from fMRI signals (Gitelman et al., 2003). Later,  
17 McLaren and colleagues proposed a “generalized PPI” approach for modeling PPI effects for more than  
18 two conditions (McLaren et al., 2012). They proposed to model each task condition with reference to all  
19 other conditions and then compared the PPI effects between the conditions of interest, rather than directly  
20 calculated PPI effects between the two conditions. Recently, we found that the interaction between not  
21 centering the psychophysiological variable and imperfect deconvolution process may lead to spurious PPI  
22 effects (Di et al., 2017), and the deconvolution may be not a necessary step for PPI analysis on block-  
23 designed data (Di and Biswal, 2017).

24 The BSC method, on the other hand, was primarily designed for event-related design (Rissman et  
25 al., 2004). By modeling the activations of every trial separately in a general linear model (GLM), one can  
26 estimate a series of beta maps for the series of trials. Therefore, connectivity in different task conditions

1 can be calculated and compared by correlations of trial-by-trial beta series variability in different  
2 conditions. The relationships between the BSC and PPI have not yet been clearly explained.  
3 Nevertheless, one study has suggested that BSC method is more suitable for event-related data than PPI  
4 (Cisler et al., 2014). However, our recent study using a large sample did not support this conclusion (Di  
5 and Biswal, 2018).

6 In the current paper, we have provided an in depth explanation of the PPI and BSC methods, and  
7 explain the relationships between these two methods. We have used both simulations and real fMRI data  
8 of an event-related designed stop signal task to illustrate the points we have made.

### 9 **1.1. Modeling of task main effects**

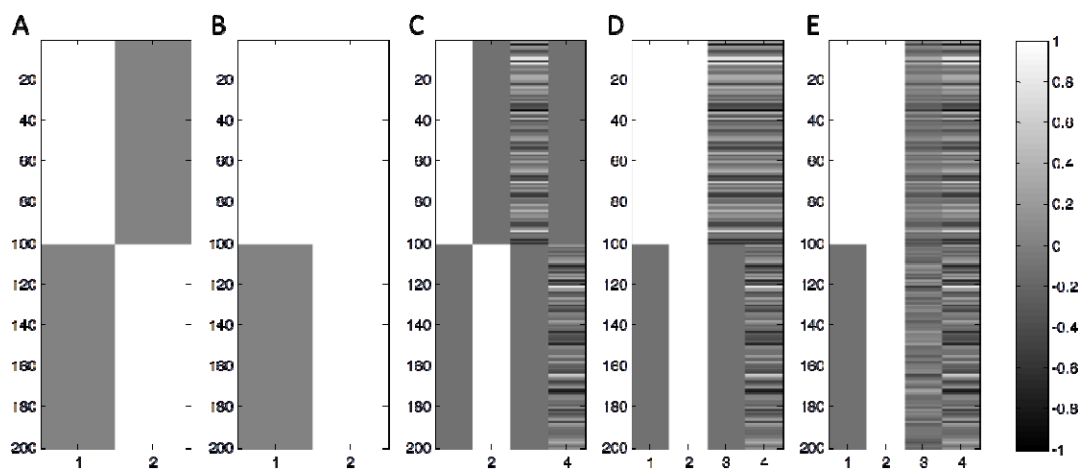
10 We start with the modeling of the main effects of task conditions. Assuming a simple task design of two  
11 conditions A and B, in a regression model, we can use two regressors to represent the two conditions in  
12 two different ways. First, we can use the two regressors to represent specific effect of each condition, i.e.  
13 using 1 to represent the modeled condition and 0 for the other condition (Figure 1A). A constant term  
14 that represents the overall effect is usually added in a regression model. Therefore, we only need to add  
15 one more regressor to represent the differential effect between the two conditions (Figure 1B). The two  
16 models are mathematically equivalent, because the two regressors in model 1A could be expressed as  
17 linear combinations of the two regressors in model 1B, and vice versa. However, because of the  
18 differences in the second regressor, the meaning of the first regressor has changed. In model 1A, each of  
19 the regressor represents the specific effect of a condition. In model 1B, the first regressor actually  
20 represents the differential effect of conditions A and B. This is important regarding the interpretation of  
21 the estimated effects of these regressors. Mathematically, model 1B can be expressed as:

$$22 \quad y = \beta_1 \cdot x_{Psych} + \beta_0 + \varepsilon \quad (1)$$

23 where  $x_{Psych}$  represents the differential effects between conditions A and B, i.e. the psychological variable.  
24 The constant term is multiplied by  $\beta_0$ , thus being omitted.  $y$  represents the brain signal in a brain region

1 or voxel.  $\beta_1$  and  $\beta_0$  are parameter estimates that represent the differential effect and mean effect of the  
2 two conditions, respectively.

3 Another important point from equation 1 is that although  $x_{Psych}$  is usually represented as 1 and 0  
4 for the two conditions, the constant component in the  $x_{Psych}$  can be explained by the constant term in  
5 equation 1 (see supplementary materials). Thus, whether centering the  $x_{Psych}$  variable will not affect the  
6 effect estimate of  $\beta_1$ , neither the interpretation of  $\beta_1$ .  $\beta_1$  always represents the differential effect of the two  
7 conditions.



8  
9 **Figure 1** Main effects and interaction models for two experimental conditions. The main effects of two  
10 conditions can be modeled as two separate regressors (A), or modeled as the differential and mean effects  
11 of the two conditions (B). When modeling the interaction terms of the experimental condition with a  
12 continuous variable, the same two strategies could be used as C and D. E illustrates how the interaction  
13 term was changed (from D) when centering the psychological variable before calculating the interaction  
14 term. Because of the different modeling strategies, the interpretations of the regressors changed.

## 16 **1.2. Functional connectivity and connectivity-task interactions**

17 The term functional connectivity was first defined by Friston (Friston, 1994) as temporal correlations  
18 between spatially remote brain regions. Assume that the functional connectivity is the same during the  
19 period of scan, e.g. resting-state, it is straightforward to calculate correlation coefficients between two

1 brain regions to represent functional connectivity. In a more general regression form, the model can be  
2 expressed as:

$$3 \quad y = \beta_1 \cdot x_{physio} + \beta_0 + \varepsilon \quad (2)$$

4 where  $x_{physio}$  represents the time series of a seed region.  $\beta_1$  in this case represents the correlation between  
5 seed and tested voxel, i.e. functional connectivity.

6 In most of task fMRI experiments, researchers design different task conditions within a scan run,  
7 so that the effect of interest becomes the differences of temporal correlations between the conditions. We  
8 can combine models 1 and 2 to include both the time series of a seed region (the physiological variable)  
9 and the psychological variable representing task designs into a regression model. Most importantly, the  
10 interaction term between the psychological and physiological variables can also be included. For the  
11 simplest scenario with only one psychological variable (two conditions), the psycho-physiological  
12 interaction (PPI) model can be expressed as:

$$13 \quad y = \beta_1 \cdot x_{Psych} + \beta_2 \cdot x_{Physio} + \beta_3 \cdot x_{Psych} \cdot x_{Physio} + \beta_0 + \varepsilon \quad (3)$$

14 Equation 3 can be illustrated figuratively in Figure 1D, with slight different orders of the variables.

15 Combine the two terms with  $x_{Physio}$ :

$$16 \quad y = \beta_1 \cdot x_{Psych} + (\beta_2 + \beta_3 \cdot x_{Psych}) \cdot x_{Physio} + \beta_0 + \varepsilon \quad (4)$$

17 Equation 4 shows that the relationship between the seed region  $x_{Physio}$  and test region  $y$  is:  $\beta_2 + \beta_3 \cdot x_{Psych}$ ,  
18 which is a linear function of  $x_{Psych}$ . Therefore, a significant  $\beta_3$  represent significant task modulations on  
19 connectivity.

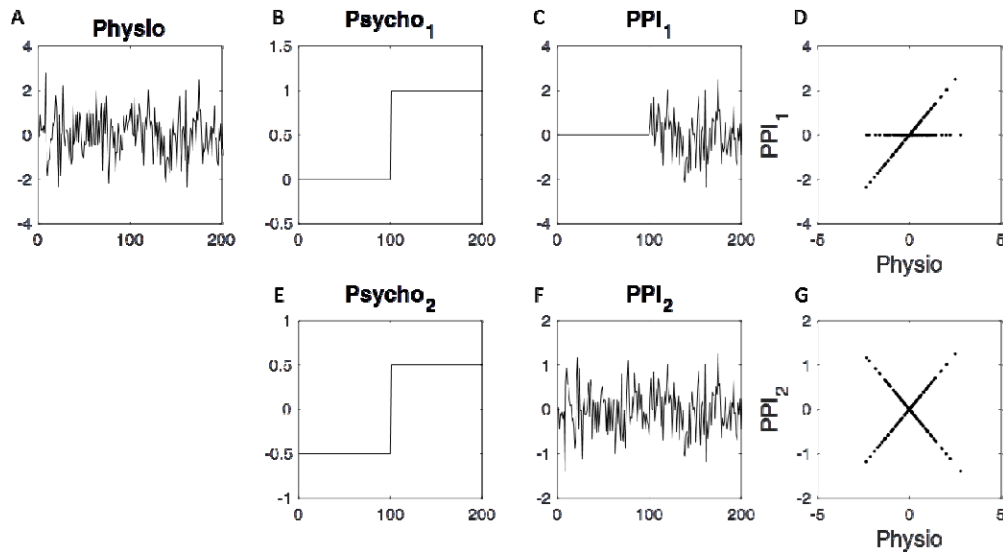
20 The interpretation of the PPI effect depends on the coding of the psychological variable.  
21 However, it also needs to consider the inclusion of other variables in the model. In equation 3 the main  
22 effect of time series  $x_{Physio}$  is included, which represents the main effect of the time series without task  
23 modulation. We can think about the time series main effect  $x_{Physio}$  and interaction effect  $x_{Physio} \cdot x_{Psych}$  as  
24 the second order counterparts of the constant effect and main effect of  $x_{Psych}$  in equation 1. Here the point

1 is that adding this time series main effect affects the interpretation of the interaction term. Because the  
2 overall relationship with the seed time series has been modeled, the interaction term measures the  
3 differences of the relationships between the two conditions. We note that if  $x_{physio}$  main effect was not  
4 added, the interaction term could actually be calculated with each condition separately (Figure 1C). Then  
5 the third and fourth columns in Figure 1C represent condition specific connectivity effects.

6 In addition, because the main effects of  $x_{physio}$  and  $x_{psych}$  are both added in the interaction model  
7 (equation 3), the interpretation of the interaction term should refer to the demeaned version of the two  
8 variables. Because the  $x_{psych}$  is usually coded as 0 and 1 for the two conditions, the demeaned version of  
9  $x_{psych}$  will be -0.5 and 0.5 instead. This will make the interaction term looked very different (column 3 in  
10 Figure 1E compared with that in Figure 1D). However, the estimated interaction effect will be identical,  
11 because the differences between the two interaction terms is the physiological main effect, which has  
12 been taken into account in the model (For real fMRI data, however, the centering matters because the  
13 main physiological main effect interacts with the deconvolution process to produce spurious PPI effects  
14 (see Di et al., 2017 for more details)).

15 To better illustrate the meaning of PPI effect, we can plot the PPI effect against the original time  
16 series  $x_{physio}$ . PPI can be represented as a projection of the seed time series, so that the PPI can represent  
17 different relationships with the seed region in different task conditions. When the psychological variable  
18 is coded as 1 and 0 for the two conditions, the PPI represents a perfect relationship with the seed time  
19 series in one condition and a smaller effect in the other, which is reflected as a horizontal line in Figure  
20 2C. When the mean of the psychological variable is removed before calculating the interaction term, the  
21 projection rotates clockwise compared with the non-centered version (Figure 2E). However, what  
22 reflected in the two projections are the same, which is the connectivity difference between the two  
23 conditions. In real cases, there may be positive connectivity in condition A and no connectivity in  
24 condition B, or there may be no connectivity in condition A but negative connectivity in condition B. In  
25 both cases, PPI can capture the differential connectivity effects. This logic is similar to the main

- 1 psychological effect explained in section 1.1, which reflects the differences between the two conditions
- 2 but not the effect in one condition.



3  
4 **Figure 2** The interaction term as a projection of the continuous (physiological) variable. A continuous  
5 variable (A) is multiplied with a psychological variable (B or E) to form an interaction term (C or F),  
6 which can be plotted against the continuous variable itself (E or G). When the psychological variable was  
7 modeled as 0 and 1 (B), the projection will result in a horizontal line ( $y = 0$ ) during the 0 period and a  $y =$   
8  $x$  line during the 1 period. But usually the psychological variable was centered (D). Therefore, the  
9 projection represent  $y = -0.5 \cdot x$  and  $y = 0.5 \cdot x$  lines during the two conditions, respectively.

10

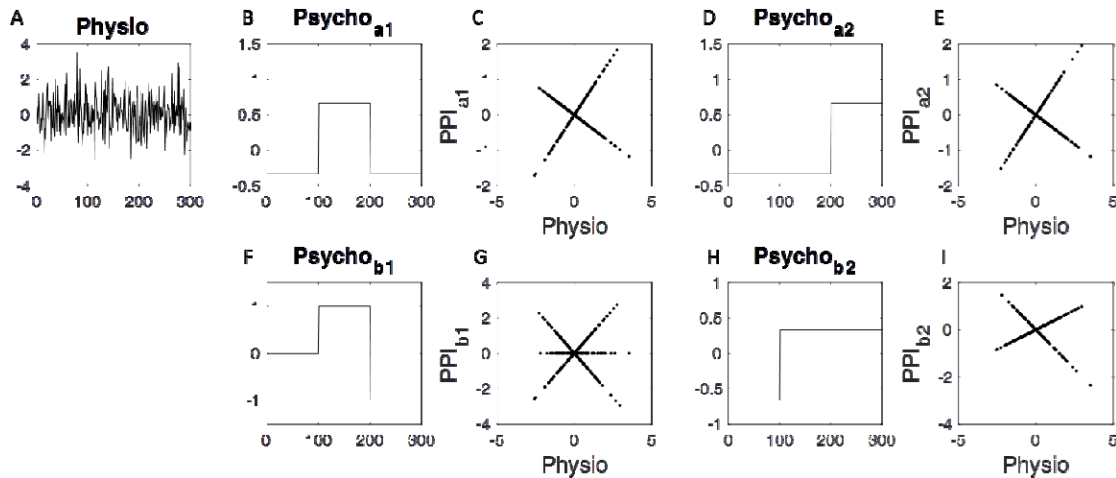
### 11 **1.3. More than two conditions**

12 When the number of conditions increases, more regressors are needed to represent each condition, with  
13 typically  $n$  regressors for  $n$  conditions. Because there is always a constant term in the regression model,  
14 we actually need  $n - 1$  additional regressors. This is convenient for most task fMRI studies, because there  
15 is usually an implicit baseline conditions in an fMRI experiment. For event-related design, it is even  
16 difficult to define the implicit baseline condition. Therefore, we can include all other experimental  
17 conditions, and leave the baseline condition out of the model. Because of the inclusion of the constant  
18 term, we should always keep in mind that the regressors included in the model represent differences of



1 between the modeled condition with respect to all other conditions, rather than the specific effect of a  
2 condition.

3 Let us assume a task design with task conditions A and B together with a baseline condition R. In  
4 this case, the effect of interest is the differences between conditions A and B. A natural way to model the  
5 three conditions is to use two regressors to represent A and B, separately (Figure 3B and 3D). We could  
6 then calculate the interaction terms of the two psychological regressors separately with the seed time  
7 series. The two interaction terms represent the correlation differences between A - (B + R) and B - (A +  
8 R), respectively. A contrast of  $[A - (B+R)] - [B - (A+R)] = 2(A - B)$  can then be used to examine the  
9 differential effect between A and B. This is usually referred to as “generalized PPI” (McLaren et al.,  
10 2012). One can also directly contrast A with B to define a new psychological variable. It can be achieved  
11 in SPM by defining contrast value 1 to condition A, and -1 to condition B. However, one should not  
12 forget that there is the third condition R, which will be implicitly left as 0. Simply doing this is  
13 problematic, because it assumes that the relationship in the R condition is somehow between what is in A  
14 and B conditions (Figure 3G). Because there are three conditions per se, we have to use two variables to  
15 model the differential effects among the three conditions. In this case, we could include one more  
16 psychological variable to represent the differential effect between the mean effect of A and B and the  
17 effect of R (Figure 3H). The interaction term of this psychological variable with the seed time series can  
18 effectively remove the differential effects of relationships between conditions A/B and condition R  
19 (Figure 3I). Therefore, if we include the PPI terms of 3H and 3I in the model, the effect of 3F will be  
20 equivalent to the differential effects of 3C and 3E. In the original paper of McLaren, it has been shown  
21 that the “generalized PPI” approach performed better than the contrast PPI. It is probably because of the  
22 neglect of the R condition. However, if the psychological variables are modeled correctly, the two  
23 methods should provide the same results.



1

2 **Figure 3** Illustrations of “generalized” PPI and contrast PPI for three conditions. Because of the inclusion

3 of the constant term, two psychological variables are needed to model the differences among the three

4 conditions. In the “generalized” PPI approach, the two psychological variables are demonstrated as B and

5 D, which represent one specific condition against the other two conditions. The corresponding PPI terms

6 were plotted against the physiological variable (A) in C and E. In the contrast PPI approach, the two

7 psychological variables are demonstrated as F and H, which represent the differential and mean effects of

8 the last two conditions. The corresponding PPI terms were plotted against the physiological variable (A)

9 in G and I.

10

#### 11 **1.4. Block design and event-related design**

12 So far we have divided the observations of different task conditions into different groups regardless of the

13 orders of the observations. For fMRI, the task conditions need to be designed carefully to accommodate

14 the properties of hemodynamic responses following neural activity changes due to the task designs.

15 There are usually two types of designs, i.e. block design and event-related design. For block design, a

16 task condition is broken into separate short blocks, and the blocks are repeated for several times within a

17 scan run. For event-related design, each trial is a unit to evoke hemodynamic responses. The temporal

18 distance between trials should be designed carefully, so that the hemodynamic response for each trial

19 could be effectively separated. The psychological variable for event-related design is modeled as a series

1 of impulse function at the onset of the trials with remaining time points as 0. The mathematical meanings  
2 of the psychological variables in a block design and an event-related design are the same, which represent  
3 the differences between conditions. And it is the same for the PPI effects. For the block design where  
4 one condition is broken into small blocks, we can still think PPI as a measure of the differences of  
5 moment-to-moment correlations between conditions. The event-related design can be thought as the  
6 correlation of activations at each trial onset time point compared with the correlation of all remaining time  
7 points. Again, it measures the differences of correlations between the two conditions but not the  
8 correlation of the trial condition itself.

9

## 10 **1.5. Convolution and deconvolution**

11 One important aspect of fMRI is the asynchrony between the (hypothetical) neuronal activity and the  
12 observed blood oxygen level dependent signals (BOLD). Imagine that a single trial elicits neural activity  
13 that is typically treated as an impulse function with short event duration. This event or short neural  
14 activity gives rise to a delayed hemodynamic response, usually called hemodynamic response function  
15 (HRF) (Figure 4A). If we have a study design or hypothetical neural activity, the observed BOLD signal  
16 can be calculated as a convolution of the neural activity time series with the HRF. Because the fMRI are  
17 discrete signals, the convolution can be converted into a multiplication of the neuronal signal with a  
18 convolution matrix defined according to the HRF. If we use  $z$  to represent variables at the neuronal level,  
19 and  $x$  to represent variables at the BOLD level, the convolution can be expressed as:

$$20 \quad x = z * h = H \cdot z \quad (5)$$

21 where  $*$  represents the convolution process, and  $\cdot$  represents matrix multiplication,  $h$  is the HRF, and  $H$   
22 represents the matrix form of  $h$ . Each column of  $H$  represents a HRF with a different start point (Figure  
23 4B). Therefore, the multiplication of a neural time series  $H$  with  $z$  can be represented as a summation of  
24 the hemodynamic responses of  $z$  at every time point.

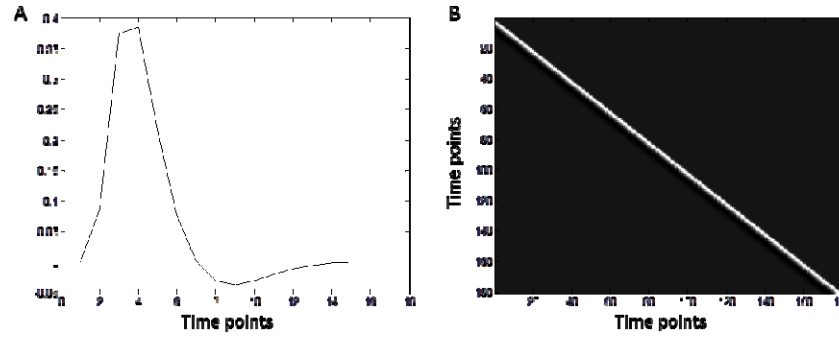


**Figure 4** Hemodynamic response function  $h$  (A) and its corresponding convolution matrix  $H$  (B).

In fMRI data analysis, we typically hypothesize that experimental manipulation will evoke immediate neural response (relative to the time scale of BOLD responses). The expected BOLD responses to the experimental manipulations could then be represented as the convolution of the psychological variable (a box-car function or a series of impulse functions) with the HRF. Thus, the BOLD level prediction variable  $x_{Psych}$  can be calculated from  $z_{Psych}$  as the following:

$$x_{Psych} = z_{Psych} * h \quad (6)$$

On the other hand, we have a time series of a region  $x_{Physio}$ , which is already at the BOLD level. Therefore, we can directly calculate the interaction term by multiplying  $x_{Physio}$  with  $x_{Psych}$ .

$$x_{PPI}^1 = x_{Psych} \cdot x_{Physio} \quad (7)$$

This is how PPI was calculated when the method was originally proposed (Friston et al., 1997). The limitation of this approach is that it calculates the interaction at the BOLD level, but the real interaction would happen at the hypothetical “neuronal” level.

Given the BOLD level time series  $x$ , we can perform the inverse process of convolution, i.e. deconvolution to recover the time series  $z$  at the neuronal level from equation 5. However, the  $H$  matrix is a square matrix, and deconvolution cannot be simply solved by inverting the  $H$  matrix. In addition, in real deconvolution problem like the fMRI signals, there are always noises in the recorded signals that

1 need to be taken into account. Therefore, the deconvolution problem has to solve the following model  
2 with a noise component  $\varepsilon$ .

$$3 \quad x = H \cdot z + \varepsilon \quad (8)$$

4 Because  $H$  cannot be directly inversed, some computational methods like regularization are needed to  
5 reliably obtain  $z$ . In SPM, it actually substitutes  $z$  with Discrete Cosine Series, so that the estimation of  
6 temporal time series was transformed into frequency domain (Gitelman et al., 2003).

7 Using deconvolution, a seed time series  $x_{physio}$  could be deconvolved to the neuronal level time  
8 series  $z_{physio}$  and multiplied with the neuronal level psychological variable. The interaction term could be  
9 convolved back into BOLD level.

$$10 \quad x_{PPI}^2 = (z_{psych} \cdot z_{physio}) * h \quad (9)$$

11 Comparing  $x_{PPI}^1$  and  $x_{PPI}^2$ , we know that they are not mathematically equivalent. The later one is more  
12 appropriate to describe neural interactions. Empirically, the PPI terms calculated with the two ways could  
13 be very similar for block-designed tasks (Di and Biswal, 2017). Deconvolution is an ill-posed problem,  
14 and relies on computational techniques, which may not work well in some circumstances. Therefore, it  
15 has been suggested that at least for block design, deconvolution may not be necessary (Di and Biswal,  
16 2017; O'Reilly et al., 2012). The deconvolution approach may still be important and necessary for event-  
17 related design.

## 18 **1.6. Beta series correlations**

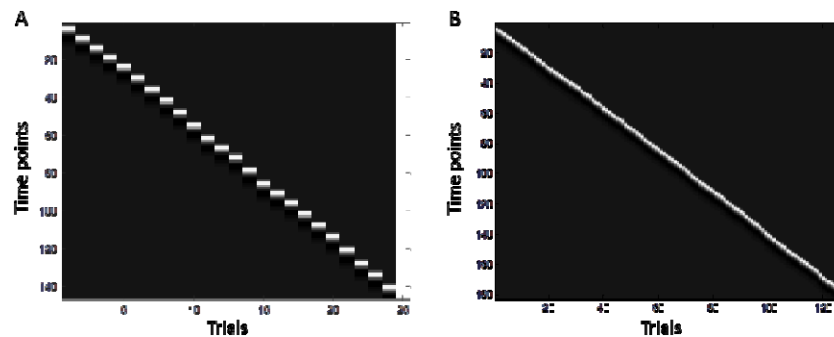
19 Beta series correlation is based on a simple idea of calculating correlations of trial-by-trial variability of  
20 activations. In order to do so, one can model each trial as a single condition by using an impulse function  
21 at the trial onset and convolve it with HRF. Therefore, in a GLM model for beta series analysis there is  
22 the same number of regressors as the number of trials plus a constant term or other effects of no interest.  
23 The model can be expressed as the following:

$$24 \quad y = \beta_1 \cdot x_1 + \beta_2 \cdot x_2 + \dots + \beta_1 \cdot x_1 + \beta_n \cdot x_n + \beta_0 + \varepsilon \quad (10)$$

1 where  $n$  represents the number of trials, and  $x_n$  represents the response of the trial  $n$ . The model can be  
2 expressed in a matrix form:

3 
$$y = X \cdot \beta + \varepsilon \quad (11)$$

4 where  $\beta$  represents a vector of  $\beta$ s that represent the activations of different trials (plus a  $\beta_0$  for the constant  
5 term). The matrix  $X$  is the design matrix (see Figure 5 for examples). One can then calculate cross-trial  
6 correlations of the beta values between regions to represent functional connectivity. Since there are  
7 usually more than one experimental condition, the beta series can be retrospectively grouped into  
8 different conditions, and the beta series correlations can be compared between the conditions.



10 **Figure 5** Example design matrices for beta series correlation (BSC) analysis for a slow event-related  
11 design (A) and a fast event-related design (B). Each regressor (column) other than the last one represents  
12 the activation of a trial, while the last column represents the constant term. The sampling time is 2 s for  
13 both of the two designs. The intertrial intervals for both the designs were randomized to optimize the  
14 estimations of hemodynamic responses. The mean intertrial intervals are 12 s for the Flanker task and 2.5  
15 s for the Stop signal task, which resulted in 24 trials and 126 trials for the two tasks, respectively.

16  
17 The hemodynamic response typically reaches the peak at 6 s after trial onset and returns back to  
18 the baseline after about 15 s. To avoid overlaps of hemodynamic responses between trials, conventional  
19 event-related experiment uses a slow fashion with intertrial interval usually greater than 10 s. Figure 5A  
20 demonstrated a beta series GLM for a slow event related design from a Flanker task (Kelly et al., 2008).  
21 Considering the sampling time of 2 s for typical fMRI, the design matrix of Figure 5A can be reliably

1 inverted (24 trial regressors vs. 146 time points). However, fast event-related design is becoming popular,  
2 because of its efficiency of maximizing experimental contrasts. The intertrial interval could be close to  
3 the sampling time of fMRI for some designs. Figure 5B demonstrated a beta series GLM for a fast event-  
4 related design from a stop signal task (Di and Biswal, 2018). In this case the mean intertrial interval is  
5 2.5 s. It can be seen from Figure 5B that the number of regressors becomes closer to the number of time  
6 points (126 trial regressors vs. 182 time points). This matrix cannot be reliably inverted using regular  
7 method, and some sophisticated computational methods may be helpful to resolve the problem, e.g. using  
8 regularization or modeling a single trial against all other trials to reduce the number of regressors  
9 (Mumford et al., 2012).

10 The beta values in the beta series model typically represent BOLD level activations at each trial.  
11 However, in an extreme case when the trials were presented at every time point, the beta series GLM  
12 model will become exactly the same as the convolution matrix in Figure 4B. This suggests a link  
13 between beta series and deconvolution. For the deconvolution model, the response for every time point  
14 was modeled (equation 8). For the beta series GLM model, however, only the time points of trial onsets  
15 were modeled (equation 11). Nevertheless, the goals of the two models are the same, i.e., to measure  
16 activity at the modeled trial onsets. Here the activations at the neuronal level at the trial onset are  
17 equivalent to the activations at the BOLD level of the trials. Therefore, we can represent beta series  
18 modeling as a modified deconvolution process, even though strictly speaking it is not. Given this, we can  
19 discuss the relationships between the PPI and BSC methods.

## 20 **1.7. The relationship between PPI and BSC**

21 As described in previous sections, the BSC method selectively picks the time points of trial onsets, and  
22 computes trial-by-trial correlations between brain regions. The PPI, on the other hand, always measures  
23 connectivity differences as coded by a psychological variable. Therefore, an absolute beta series  
24 correlation in one condition is not directly comparable to a PPI effect. However, what are usually of  
25 interest are the connectivity differences between conditions. In this case, we can compare beta series  
26 correlation differences between conditions. Considering the same task design with experimental

1 conditions A and B and a baseline R, we can directly compare the beta series correlations between  
2 conditions A and B (i.e.,  $A - B$ ). If PPI was modeled using the “generalized” approach, we can have the  
3 two PPI effects representing  $A - (B + R)$  and  $B - (A + R)$ . These two PPI effects can be directly  
4 contrasted, which resulted in the contrast of  $2 \cdot (A - B)$ . Therefore, in theory the BSC and PPI methods  
5 measure the same connectivity differences.

6 Although theoretically PPI and BSC could measure the same task modulated connectivity, the  
7 results of PPI and BSC on real fMRI data may not be identical. Several factors may contribute to the  
8 differences. The first is the different approach to deconvolution. The deconvolution method  
9 implemented in SPM uses Discrete Cosine Series to convert the temporal domain signal into frequency  
10 domain, and then applies regularization on the frequency domain to suppress high frequency components  
11 in the signals. For BSC method, if it is a slow event-related design, the design matrix may be easy to be  
12 reliably inverted without using computational techniques. For a fast event-related design, some  
13 regularization method may be used obtain beta series, or the model should be modified to contain one  
14 regressor of one trial and one regressor of all other trials to reduce the number of regressors (Mumford et  
15 al., 2012). The efficiency and reliability of these mentioned methods are difficult to determine and  
16 compare. Therefore it is difficult to make a definite conclusion about which method is better over the  
17 other.

18 By using a regression model PPI measures covariance differences between conditions. On the  
19 other hand, BSC typically uses correlation coefficients. It is still largely unknown how the variability of  
20 BOLD signals changes in different task conditions. But the differences in measures of covariance and  
21 correlations can certainly give different results. For BSC, one can choose different measures of  
22 connectivity, e.g. Pearson product-moment correlation, Spearman rank correlation, and covariance, or  
23 even use similar beta series by task interaction to estimate connectivity differences. However, it is still an  
24 open question about which method is optimal for the purpose of connectivity estimation.

## 25 **1.8. An empirical demonstration**



1 To summarize, we have explained the meanings of PPI and BSC analyses, as well as the relationships  
2 between the two methods. PPI always measures connectivity differences as coded by the psychological  
3 variable, while BSC could measure connectivity in specific condition. When comparing connectivity  
4 between conditions, PPI and BSC methods should in principle generate similar results, although different  
5 ways to handle deconvolution and different measures of connectivity may contribute to the differences in  
6 results. For PPI analysis, there may be multiple ways to model task conditions in PPI analysis. But if  
7 done correctly, different approaches in principle should generate the same results.

8 In the following sections, we describe PPI and BSC analyses on a fast event-related designed stop  
9 signal task. In this task there were two experimental conditions (Go and Stop) in addition to an implicit  
10 baseline. The connectivity differences between the Stop and Go conditions have been reported in our  
11 previous work (Di and Biswal, 2018). To better illustrate the relationships between PPI and BSC  
12 methods, we reported connectivity measures of PPI and BSC methods for simple conditions and condition  
13 differences. In addition, we will compare different measures of BSC, i.e. Pearson's correlation,  
14 Spearman's correlation, and covariance, and examine whether these measures will affect BSC results.  
15 Lastly, we will compare PPI results using the "generalized PPI" approach with direct contrast approach  
16 where the differential and mean effects of the two conditions are both modeled. We will show that these  
17 two modeling approaches can provide almost identical connectivity difference measures.

18

## 19 **2. Materials and methods**

### 20 **2.1. Dataset and designs**

21 In a previous study, we have reported PPI and BSC results of connectivity differences between the Stop  
22 and Go conditions (Di and Biswal, 2018). In the current manuscript, we have used the same data to  
23 illustrate how different PPI models could give rise to the same results and how the PPI and BSC methods  
24 can be similar or different. This dataset was obtained from the OpenfMRI database, with accession  
25 number ds000030. Only healthy subjects' data were included in the current analysis. After removing  
26 subjects due to large head motion, a total of 114 subjects were included in the current analysis (52

1 females). The mean age of the subjects was 31.1 years (range from 21 to 50 years). In the stop signal  
2 task, the subjects have to indicate the direction (left or right) of an arrow presented in the center of the  
3 screen. For one fourth of the trials, a 500 Hz tone was played shortly after the arrow, which signaled the  
4 subjects to withdraw their response. In a single fMRI run, there were 128 trials in total in total, with 96  
5 Go trials and 32 Stop trials. The task used a fast event-related design, with a mean intertrial interval of  
6 2.5 s (range from 2 s to 5.5 s).

7 The fMRI data were collected using a T2\*-weighted echoplanar imaging (EPI) sequence with the  
8 following parameters: TR = 2000 ms, TE = 30 ms, FA = 90 deg, matrix  $64 \times 64$ , FOV = 192 mm; slice  
9 thickness = 4 mm, slice number = 34. 184 fMRI images were acquired for each subject. The T1  
10 weighted structural images were collected using the following parameters: TR = 1900 ms, TE = 2.26 ms,  
11 FOV = 250 mm, matrix =  $256 \times 256$ , sagittal plane, slice thickness = 1 mm, slice number = 176. More  
12 information about the data can be found in (Poldrack et al., 2016).

### 13 **2.2. fMRI preprocessing**

14 The fMRI image processing and analysis were performed using SPM12 (v6685)  
15 (<http://www.fil.ion.ucl.ac.uk/spm/>) and MATLAB codes in MATLAB R2013b environment  
16 (<https://www.mathworks.com/>). The anatomical image for each subject was first segmented, and  
17 normalized to standard MNI (Montreal Neurological Institute) space. The first two functional images  
18 were discarded, and the remaining 182 images were realigned to the first image, and coregistered to the  
19 subject's own anatomical image. The functional images were then transformed into MNI space by using  
20 the deformation images derived from the segmentation step, and were spatially smoothed using a 8 mm  
21 FWHM (full width at half maximum) Gaussian kernel.

### 22 **2.3. PPI analysis**

23 The first step of PPI analysis is to build a GLM model of task regressor, which can also be used to obtain  
24 task related activations. In the current analysis, the Go and Stop conditions were modeled separately as  
25 series of events. In SPM, the durations of the events are usually set as 0 to reflect the impulse nature of  
26 the events. But for PPI analysis, the problem is that after deconvolution, the time series were up-sampled

1 (16 times by default). If the duration was set as 0, then the neuronal level psychological variable only has  
2 a time bin of TR/16 of one, leaving all other time bins as 0. This may be problematic when multiplying  
3 this psychological variable with the deconvolved seed time series. Considering that the calculated PPI  
4 term will be convolved back with HRF, which resembles a low pass filtering, the effects of trial duration  
5 may not be that significant. In the previous analysis, we set the duration to 1.5 s, which is the actual  
6 duration of the trial. We have also shown in the supplementary materials that setting the event duration as  
7 0 produce very similar results as those with 1.5 s duration. In addition to the two task variables, 24 head  
8 motion regressors and one constant regressor were also included in the GLM model. After model  
9 estimation, the times series from 164 ROIs were extracted. The head motion, constant, and low frequency  
10 drift effects were adjusted during the ROI time series extraction.

11 The PPI terms were calculated using the two different approaches, i.e. “generalized” PPI and  
12 contrast PPI. In the first approach, we first used the contrasts [1 0] and [0 1] to define two psychological  
13 variable to represent the Go and Stop conditions, separately. The PPI terms were then calculated  
14 accordingly using the deconvolution method. The calculated PPI terms were combined together with the  
15 original model to form a new GLM model for PPI analysis:

$$16 \quad y = \beta_1 \cdot x_{Go} + \beta_2 \cdot x_{Stop} + \beta_3 \cdot x_{ROI} + \beta_4 \cdot x_{PPI:Go} + \beta_5 \cdot x_{PPI:Stop} + \beta_0 + \varepsilon \quad (12)$$

17 This model included one constant term, two regressors of task activations of the Go and Stop condition,  
18 one regressor of the time series of a seed region, and two regressors of PPIs. Because the dependent  
19 variable  $y$  is also a ROI time series, where the head motion effects have already been removed, the head  
20 motion regressors were no longer included in the PPI models. After model estimation, we calculated  $\beta_5 -$   
21  $\beta_4$  as the connectivity effects between the Stop and Go conditions.

22 We also applied the second model where the differential and mean effects of the Stop and Go  
23 conditions were modeled. The differential effect was defined using the contrast [-1 1], and the mean  
24 effect was defined using the contrast [1/2 1/2]. The GLM for the contrast PPI analysis was as follow:

$$25 \quad y = \beta_1 \cdot x_{Go+Stop} + \beta_2 \cdot x_{Stop-Go} + \beta_3 \cdot x_{ROI} + \beta_4 \cdot x_{PPI:Go+Stop} + \beta_5 \cdot x_{PPI:Stop-Go} + \beta_0 + \varepsilon \quad (13)$$

1 The  $\beta_5$  could be used for group level analysis to present connectivity differences between the Stop and Go  
2 conditions.

3 For each subject, the PPI models were built for each ROI, and were fitted to all other ROIs. The  
4 beta estimates of interest or contrast of interest were calculated between each pair of ROI, which yielded a  
5 164 by 164 matrix for each effect. The matrices were transposed and averaged with the original matrices,  
6 which yielded symmetrical matrices. One sample t test was performed on each element of the matrix for  
7 an effect of interest. False discovery rate (FDR) correction was used at  $p < 0.05$  to identify statistical  
8 significant effects in a total of 13,366 effects ( $164 \times (164 - 1) / 2$ ).

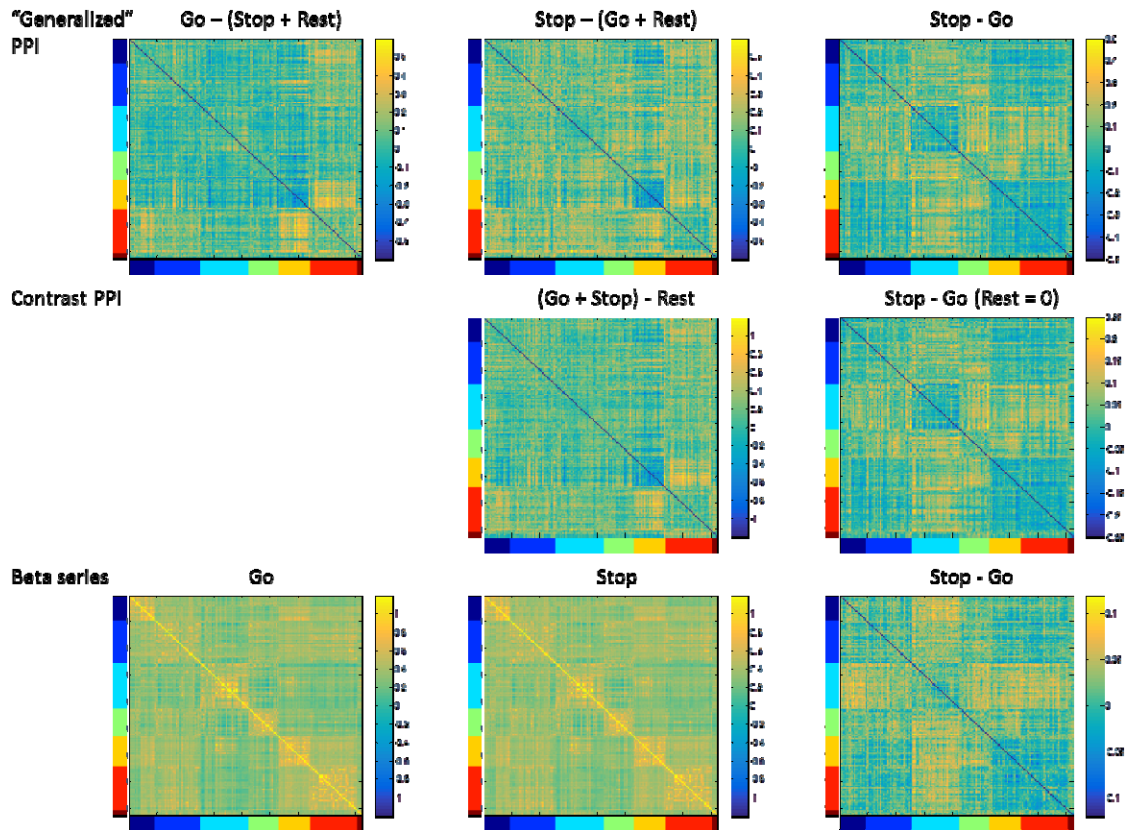
#### 9 **2.4. Beta series analysis**

10 As has been shown in our previous paper (Di and Biswal, 2018), modeling all trials together in a single  
11 model could not work for the beta series analysis. Therefore, we only reported the results from the single-  
12 trial-versus-other-trials method (Mumford et al., 2012). We first built a GLM model for each trial, where  
13 the first regressor represented the activation of the specific trial and the second regressor represented the  
14 activations of all the remaining trials. The 24 head motion parameters were also included in the GLMs as  
15 covariance. The duration of events was set as 0. After model estimation, beta values of each ROI were  
16 extracted for each trial. The beta series of each ROI were sorted into the two conditions, and connectivity  
17 measures across the 164 ROIs were calculated. In our previous work, we used Spearman's rank  
18 coefficients to avoid the assumption of Gaussian distribution of beta values or spurious correlations due to  
19 outliers. In the current analysis, we also calculated Pearson's correlation coefficients and covariance to  
20 examine whether these two measures may give more reliable estimates of connectivity. Before  
21 calculating the covariance, the whole beta series (Go and Stop together) of a ROI were z transformed. All  
22 the three measures yielded a symmetrical matrix for each subject. The correlation matrices (either  
23 Pearson's or Spearman's) were transformed into Fisher's z matrices. For a single condition, mean of  
24 Fisher's z values or covariance values were averaged across subjects. Paired t test was also performed to  
25 compare the differences between the two conditions at every element in the matrix. A FDR correction at  
26  $p < 0.05$  was used to identify statistical significant effects.

1

### 2 **3. Results**

3 Figure 6 demonstrates the PPI and BSC effects across the 164 ROIs in the Go and Stop conditions, as  
4 well as the differences between the two conditions. To show the overall effects, the matrices were not  
5 thresholded. For the “generalized PPI” model, both the Go and Stop condition had greater connectivity  
6 compared with the respective control conditions, mainly between visual and sensorimotor regions and  
7 between cerebellar and sensorimotor regions. The Stop condition additionally showed widespread  
8 connectivity increases, which resulted in different connectivity between the Stop and Go conditions in  
9 many connections. For the direct contrast PPI model, the mean effect of Go and Stop trials compared  
10 with the baseline were very similar to the single PPI effects of the two conditions separately. And the  
11 differential effects of the Stop and Go conditions are very similar to the contrast of Stop and Go PPI  
12 effects from the “generalized PPI” model. In contrast, the beta series correlations for the Go and Stop  
13 trials separately did not show similar patterns as the simple PPI effects in the “generalized PPI” models.  
14 The correlation matrices are indeed similar to resting-state correlations. However, despite the differences  
15 of effects in the single condition, the differential effects between the Stop and Go conditions are similar  
16 for the two PPI models as well as the BSC. This is consistent with our theoretical explanations of these  
17 methods.



1

2

**Figure 6** Psychophysiological interaction (PPI) and beta series correlation (BSC) results from the stop

3

signal task. The top row showed the PPI matrices using the “generalized PPI” model, where the Go

4

condition and Stop condition were modeled separately. The middle row showed the PPI matrices using

5

direct contrast of the Go and Stop conditions. The bottom row showed correlation matrices using the beta

6

series method. The right-side color scales of all matrices were made sure to be positive and negative

7

symmetrical, but the range was adjusted based on the values in each matrix. The left and bottom color

8

bars indicate the seven functional modules, including cerebellar, cingulo-opercular, default mode, fronto-

9

parietal, occipital, sensorimotor, and emotion modules from dark blue to dark red.

10

11

The connectivity differences between the Stop and Go conditions have been reported previously

12

(Di and Biswal, 2018). Here we only focus on the effect of task execution, i.e. the mean effect of the Go

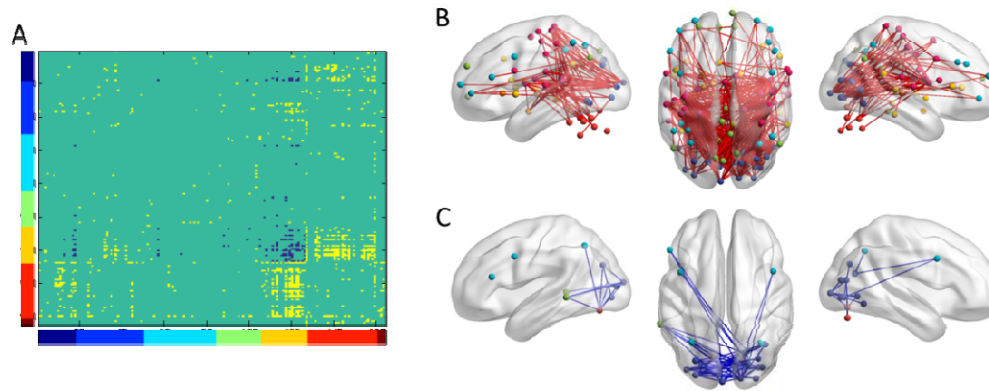
13

the Stop conditions compared with the baseline. Statistical significant effects were thresholded at  $p <$

14

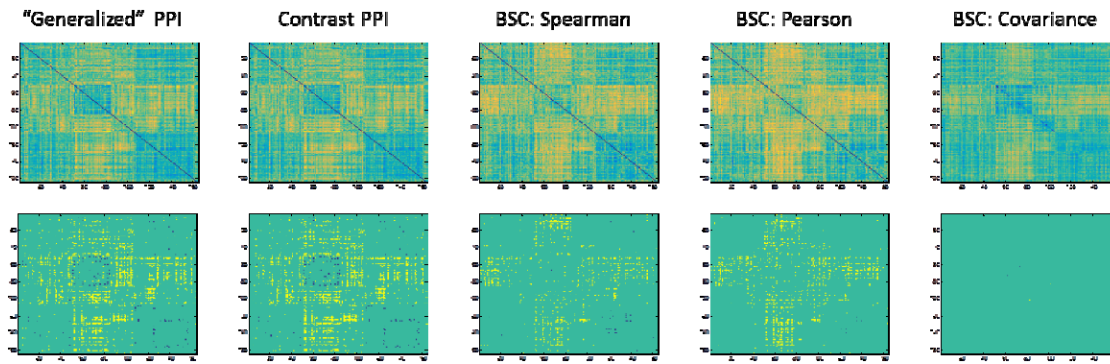
0.05 (FDR corrected) and visualized using BrainNet Viewer (Xia et al., 2013) (Figure 7). It is clearly

1 shown that there was reduced connectivity within the visual areas, and increased connectivity mainly  
2 between visual regions and sensorimotor regions and between visual regions and other brain regions such  
3 as cingulo-opercular regions.



4  
5 **Figure 7** Mean PPI effects of the Go and Stop trials compared with the implicit baseline. A shows the  
6 thresholded PPI matrix at  $p < 0.05$  of FDR (false discovery rate) correction. Yellow represents positive  
7 PPI effects, while blue represents negative effects. The color bars indicate the seven functional modules,  
8 including cerebellar, cingulo-opercular, default mode, fronto-parietal, occipital, sensorimotor, and  
9 emotion modules from dark blue to dark red. B and C show the positive and negative effects on a brain  
10 model using BrainNet Viewer.

11  
12 Lastly, for the contrast of Stop vs. Go where the two PPI models and BSC yielded similar results,  
13 we compared the BSC results with different methods with the PPI results (Figure 8). The significant  
14 effects of the “generalized PPI” and contrast PPI were almost identical. When comparing the three  
15 measures of Spearman’s correlation, Pearson’s correlation, and covariance, Pearson’s correlation  
16 produced more significant effects than Spearman’s correlation. And covariance differences only showed  
17 one positive and one negative significant effect. However, even the results from Pearson’s correlation  
18 showed less significant results than the two PPI models.



1

2

**Figure 8** Unthresholded (upper row) and thresholded (lower row) matrices of task modulated

3

connectivity between the Stop and Go conditions estimated by different methods. A  $p < 0.05$  of false

4

discovery rate (FDR) correction was used to threshold each matrix. The color scales of all matrices were

5

made sure to be positive and negative symmetrical. But the range was adjusted based on the values in

6

each matrix.

7

#### 8 **4. Discussion**

9

In the current paper, we have compared between PPI and BSC, and explained that because the inclusion

10

of the physiological variable in the PPI model, a PPI effect always represents the differences of

11

correlations between conditions. In contrast, BSC can measure correlations in a specific task condition.

12

However, when comparing between conditions, PPI and BSC methods should in principle yield similar

13

estimates of connectivity differences. The results of PPI and BSC analyses on a real event-related

14

designed stop signal task agree with our theoretical explanation of the two methods. Firstly, PPI always

15

conveyed connectivity differences between conditions, even when using a simple psychological variable

16

of 1s and 0s. The direct contrast PPI could show the same results as “generalized PPI” when the

17

conditions were modeled properly. Secondly, we showed that simple correlations of beta series in one

18

condition reflected the absolute effects of connectivity, which resembled resting-state connectivity.

19

However, when the effects were contrasted between conditions, the PPI and BSC results turned out to be

20

very similar.



1           The simple BSC correlation for the Go and Stop conditions are very similar to each other, and are  
2 also similar to what we typically observed in resting-state. They all show square like structures along the  
3 diagonal, which reflects higher functional connectivity within the predefined functional modules and  
4 lower functional connectivity between regions from different functional modules. This is consistent with  
5 the observation that correlations in many different task conditions are very similar (Cole et al., 2014). But  
6 the fact that the absolute BSC correlations in a task condition resemble resting-state connectivity makes  
7 their functional implications on the task conditions limited. On the other hand, for PPI analysis even the  
8 simple PPI effects of one condition yield connectivity differences between the very condition and the rest  
9 of the time points. In the current analysis, we demonstrate the task modulated connectivity of the Go and  
10 Stop conditions compared with their respective baseline. But this cannot be achieved by using the BSC  
11 method, because the implicit baseline conditions cannot be easily modeled in the BSC model.

12           The connectivity differences between the Go or Stop conditions compared with their respective  
13 baseline suggested changes of connectivity related to general task executions. This contrast revealed  
14 decreased connectivity between visual areas, and increased connectivity between visual areas and  
15 sensorimotor areas among other brain regions. The reduced connectivity within the visual areas during  
16 task execution compared with baseline is consistent with our previous studies using a set of different tasks  
17 (Di et al., 2017) as well as in a simple checkerboard task (Di and Biswal, 2017). However, in contrast to  
18 reduced functional connectivity between visual and sensorimotor regions in the checkerboard task (Di and  
19 Biswal, 2017), the current results showed increased connectivity between the visual and sensorimotor  
20 regions. It is not surprising because the stop signal task requires the subjects to respond to visual stimuli,  
21 therefore yield increased functional coupling between visual and sensorimotor regions.

22           When directly comparing the differences between the Stop and Go conditions, all the PPI and  
23 BSC methods showed similar results. First, the “generalized PPI” and contrast PPI showed almost  
24 identical results. It is not surprising given that we have explained they are mathematically identical.  
25 Although we think that the “generalized PPI” is still a better strategy to model PPI effects, in some  
26 circumstances the direct contrast method may be useful. For example, if there are many task conditions

1 designed (say conditions A, B, C, D, and E, plus a baseline condition R), but eventually there is only one  
2 contrast of interest (A vs. B). In this case, there is no need to model PPI effects of the five conditions  
3 separately. One can model the mean effects of A and B against all other conditions and the contrast effect  
4 between A and B leaving all other conditions as 0. In this way, the direct contrast method is more flexible  
5 in terms of defining psychological variables and contrasts.

6 As has been reported in our previous paper, BSC differences can yield similar connectivity  
7 differences when compared between the Stop and Go conditions (Di and Biswal, 2018). In the current  
8 analysis, we further compared BSC differences results using Pearson's correlation and covariance. The  
9 unthresholded matrices of the three connectivity measures were very similar. When performing statistical  
10 inferences using a  $p < 0.05$  threshold of FDR correction, Pearson's correlation yielded more statistical  
11 significant effects than Spearman's correlation, while covariance could only show two statistical  
12 significant effects. The numbers of statistical significant effects were all smaller than those in the PPI  
13 analyses. Mathematically, the PPI effect is more similar to the differences of covariance between  
14 conditions than the other correlation measures. However, the covariance differences of beta series failed  
15 to convey as many significant results than the other correlations measures. It is probably due to that the  
16 BSC model for the stop signal task is not reliable enough, so that there are large amount of spurious trial-  
17 by-trial variability that need to be standardized before calculating covariance.

18 In this paper, we have explained the relationships between PPI and BSC, and showed that in  
19 principle these two methods should measure the same connectivity differences between conditions.  
20 However, PPI and BSC methods could yield slightly different results mainly due to the different ways of  
21 dealing with deconvolution or trail-by-trial activation estimates. Because of this, simply comparing the  
22 two methods is less of interest. Further studies may focus on deconvolution techniques such that the  
23 results of both PPI and BSC could improve. For example, more sophisticated filters could be used for  
24 deconvolution, e.g. cubature Kalman filtering (Havlicek et al., 2011). In addition, applying subject  
25 specific HRF (Pedregosa et al., 2015) may be helpful for both PPI and BSC methods. Lastly, the  
26 effectiveness of the two methods may also depend on the temporal distance of trials. Although the

1 current study showed that both of the methods could work for the fast event-related stop signal task, it is  
2 reasonable to speculate that these two methods may work better when trial distances are larger. The  
3 fitness of the two methods on different design parameters warrants further investigations.

4

5

6 **Reference:**

7 Biswal, B., Yetkin, F.Z., Haughton, V.M., Hyde, J.S., 1995. Functional connectivity in the motor cortex  
8 of resting human brain using echo-planar MRI. *Magn. Reson. Med.* 34, 537–41.  
9 doi:10.1002/mrm.1910340409

10 Biswal, B.B., Mennes, M., Zuo, X.-N., Gohel, S., Kelly, C., Smith, S.M., Beckmann, C.F., Adelstein, J.S.,  
11 Buckner, R.L., Colcombe, S., Dogonowski, A.-M., Ernst, M., Fair, D., Hampson, M., Hoptman,  
12 M.J., Hyde, J.S., Kiviniemi, V.J., Kötter, R., Li, S.-J., Lin, C.-P., Lowe, M.J., Mackay, C., Madden,  
13 D.J., Madsen, K.H., Margulies, D.S., Mayberg, H.S., McMahon, K., Monk, C.S., Mostofsky, S.H.,  
14 Nagel, B.J., Pekar, J.J., Peltier, S.J., Petersen, S.E., Riedl, V., Rombouts, S.A.R.B., Rypma, B.,  
15 Schlaggar, B.L., Schmidt, S., Seidler, R.D., Siegle, G.J., Sorg, C., Teng, G.-J., Veijola, J., Villringer,  
16 A., Walter, M., Wang, L., Weng, X.-C., Whitfield-Gabrieli, S., Williamson, P., Windischberger, C.,  
17 Zang, Y.-F., Zhang, H.-Y., Castellanos, F.X., Milham, M.P., 2010. Toward discovery science of  
18 human brain function. *Proc. Natl. Acad. Sci. U. S. A.* 107, 4734–9. doi:10.1073/pnas.0911855107

19 Cisler, J.M., Bush, K., Steele, J.S., 2014. A comparison of statistical methods for detecting context-  
20 modulated functional connectivity in fMRI. *Neuroimage* 84, 1042–1052.

21 doi:10.1016/j.neuroimage.2013.09.018

22 Cole, M.W., Bassett, D.S., Power, J.D., Braver, T.S., Petersen, S.E., 2014. Intrinsic and task-evoked  
23 network architectures of the human brain. *Neuron* 83, 238–251. doi:10.1016/j.neuron.2014.05.014

24 Di, X., Biswal, B.B., 2017. Psychophysiological Interactions in a Visual Checkerboard Task:  
25 Reproducibility, Reliability, and the Effects of Deconvolution. *Front Neurosci* 1–36.

26 doi:10.3389/fnins.2017.00573

- 1 Di, X., Biswal, B.B., 2018. Toward Task Connectomics: Examining Whole-Brain Task Modulated  
2 Connectivity in Different Task Domains. *Cereb Cortex*.
- 3 Di, X., Reynolds, R.C., Biswal, B.B., 2017. Imperfect (de)convolution may introduce spurious  
4 psychophysiological interactions and how to avoid it. *Hum. Brain Mapp.* 38, 1723–1740.  
5 doi:10.1002/hbm.23413
- 6 Friston, K.J., 1994. Functional and effective connectivity in neuroimaging: A synthesis. *Hum. Brain*  
7 *Mapp.* 2, 56–78. doi:10.1002/hbm.460020107
- 8 Friston, K.J., Buechel, C., Fink, G.R., Morris, J., Rolls, E., Dolan, R.J., 1997. Psychophysiological and  
9 modulatory interactions in neuroimaging. *Neuroimage* 6, 218–29.
- 10 Friston, K.J., Harrison, L., Penny, W., 2003. Dynamic causal modelling. *Neuroimage* 19, 1273–1302.  
11 doi:10.1016/S1053-8119(03)00202-7
- 12 Gitelman, D.R., Penny, W.D., Ashburner, J., Friston, K.J., 2003. Modeling regional and  
13 psychophysiological interactions in fMRI: the importance of hemodynamic deconvolution.  
14 *Neuroimage* 19, 200–7.
- 15 Havlicek, M., Friston, K.J., Jan, J., Brazdil, M., Calhoun, V.D., 2011. Dynamic modeling of neuronal  
16 responses in fMRI using cubature Kalman filtering. *Neuroimage* 56, 2109–2128.  
17 doi:10.1016/j.neuroimage.2011.03.005
- 18 Kelly, A.M.C., Uddin, L.Q., Biswal, B.B., Castellanos, F.X., Milham, M.P., 2008. Competition between  
19 functional brain networks mediates behavioral variability. *Neuroimage* 39, 527–37.  
20 doi:10.1016/j.neuroimage.2007.08.008
- 21 McLaren, D.G., Ries, M.L., Xu, G., Johnson, S.C., 2012. A generalized form of context-dependent  
22 psychophysiological interactions (gPPI): A comparison to standard approaches. *Neuroimage* 61,  
23 1277–1286. doi:10.1016/j.neuroimage.2012.03.068
- 24 Mumford, J.A., Turner, B.O., Ashby, F.G., Poldrack, R.A., 2012. Deconvolving BOLD activation in  
25 event-related designs for multivoxel pattern classification analyses. *Neuroimage* 59, 2636–2643.  
26 doi:10.1016/j.neuroimage.2011.08.076

- 1 O'Reilly, J.X., Woolrich, M.W., Behrens, T.E.J., Smith, S.M., Johansen-Berg, H., 2012. Tools of the  
2 Trade: Psychophysiological Interactions and Functional Connectivity. *Soc. Cogn. Affect. Neurosci.*  
3 nss055-. doi:10.1093/scan/nss055
- 4 Pedregosa, F., Eickenberg, M., Ciuciu, P., Thirion, B., Gramfort, A., 2015. Data-driven HRF estimation  
5 for encoding and decoding models. *Neuroimage* 104, 209–220.  
6 doi:10.1016/j.neuroimage.2014.09.060
- 7 Poldrack, R.A., Congdon, E., Triplett, W., Gorgolewski, K.J., Karlsgodt, K.H., Mumford, J.A., Sabb,  
8 F.W., Freimer, N.B., London, E.D., Cannon, T.D., Bilder, R.M., 2016. A phenome-wide  
9 examination of neural and cognitive function. *Sci. Data* 3, 160110. doi:10.1038/sdata.2016.110
- 10 Rissman, J., Gazzaley, A., D'Esposito, M., 2004. Measuring functional connectivity during distinct stages  
11 of a cognitive task. *Neuroimage* 23, 752–63. doi:10.1016/j.neuroimage.2004.06.035
- 12 Xia, M., Wang, J., He, Y., 2013. BrainNet Viewer: a network visualization tool for human brain  
13 connectomics. *PLoS One* 8, e68910. doi:10.1371/journal.pone.0068910
- 14